

Magnetic depth profile of a modulation-doped $\text{La}_{1-x}\text{Ca}_x\text{MnO}_3$ exchange-biased system

A. Hoffmann,^{1,2,*} S. J. May,¹ S. G. E. te Velthuis,¹ S. Park,^{3,4} M. R. Fitzsimmons,³ G. Campillo,^{5,6} and M. E. Gómez⁵

¹Materials Science Division, Argonne National Laboratory, Argonne, Illinois 60439, USA

²Center for Nanoscale Materials, Argonne National Laboratory, Argonne, Illinois 60439, USA

³Los Alamos National Laboratory, Los Alamos, New Mexico 87545, USA

⁴Department of Physics, Pusan National University, Busan 609-735, Korea

⁵Department of Physics, Universidad del Valle, A.A. 25360, Cali, Colombia

⁶Instituto de Física, Universidad de Antioquia, A.A. 1226, Medellín, Colombia

(Received 1 April 2009; revised manuscript received 28 July 2009; published 17 August 2009)

Recent magnetometry measurements in modulation-doped $\text{La}_{1-x}\text{Ca}_x\text{MnO}_3$ suggested that a net magnetization extends from the ferromagnetic layers into the adjacent antiferromagnetic layers. Here we test this hypothesis by polarized neutron reflectometry, which allows us to determine the depth resolved magnetization profile. From fits to the reflectivity data we find that the additional magnetization does not occur at the ferromagnetic/antiferromagnetic interfaces, but rather in a thin region of the first antiferromagnetic layer adjacent to the interface with the substrate.

DOI: [10.1103/PhysRevB.80.052403](https://doi.org/10.1103/PhysRevB.80.052403)

PACS number(s): 75.25.+z, 75.47.Lx, 75.70.Cn

Understanding the properties of complex oxide heterostructures is a challenging research problem due to the intricate interplay between spin, charge, orbital, and structural degrees of freedom.¹ At the same time the unexpected electronic and other physical properties that emerge at the interfaces of complex oxide heterostructures open up promising avenues for advanced functional materials.² A basic challenge throughout the investigation of interfaces in oxide heterostructures is the characterization of their properties with techniques that provide sufficient depth resolution even for deeply buried interfaces far away from the sample surface. To this end magnetically ordered complex oxide materials provide very useful model systems, since the depth variations of a ferromagnetic magnetization are readily accessible with very high resolution (up to a single monolayer) through polarized neutron reflectometry.^{3–10} Furthermore, the depth-dependent magnetization structure may reflect changes of the underlying electronic structure caused by charge transfer at the interfaces of two different oxide materials.⁶

Some of the more thoroughly studied magnetic heterostructures are exchange-bias systems,^{11,12} where the coupling between an antiferromagnet and a ferromagnet results in an asymmetric hysteresis loop shift. Mixed valence manganese heterostructures with modulated composition are a particularly interesting realization of exchange-bias systems,^{13–16} since the magnetic order in these materials can be tuned via cation doping, which shifts the balance from antiferromagnetic superexchange to ferromagnetic double exchange coupling.¹⁷ Thus in an exchange-bias system consisting of differently doped antiferromagnetic and ferromagnetic manganese layers all the spins occupy the same lattice sites, but only their interaction is varied by local doping. However, it is clear that the electronic structure at interfaces can be more complex due to charge transfer^{6,18} and therefore it is not obvious that the magnetic antiferromagnetic/ferromagnetic interface indeed closely follows the chemical doping. In fact, recent experiments in modulation-doped $\text{La}_{1-x}\text{Ca}_x\text{MnO}_3$ superlattices ($x=1/3$ and $2/3$ for ferromagnetic and antiferromagnetic ordering, respectively) showed that the saturation magnetization of these superlattices depends on the thickness

of the antiferromagnetic layer, and, if normalized by the nominal thickness of the ferromagnetic layer, the saturation magnetization can even exceed bulk values for $\text{La}_{2/3}\text{Ca}_{1/3}\text{MnO}_3$.¹⁶ This suggests that the ferromagnetic magnetization may extend beyond the chemical doping interface into the antiferromagnetic layer. In order to test this hypothesis we performed polarized neutron reflectometry on a $\text{La}_{2/3}\text{Ca}_{1/3}\text{MnO}_3/\text{La}_{1/3}\text{Ca}_{2/3}\text{MnO}_3$ superlattice and found that the magnetization profile is in general commensurate with the doping profile, but surprisingly an additional layer with net ferromagnetic magnetization is formed at the interface between the first nominally antiferromagnetic $\text{La}_{1/3}\text{Ca}_{2/3}\text{MnO}_3$ layer with the SrTiO_3 substrate.

The superlattice was grown on a (100) SrTiO_3 single-crystal substrate by high-oxygen pressure (3.5 mbars) sputtering at a substrate temperature of 850 °C using bulk stoichiometric antiferromagnetic $\text{La}_{1/3}\text{Ca}_{2/3}\text{MnO}_3$ and ferromagnetic $\text{La}_{2/3}\text{Ca}_{1/3}\text{MnO}_3$ targets.¹⁹ The superlattice consisted of ten repetitions of 40 unit cells (156 Å) of $\text{La}_{1/3}\text{Ca}_{2/3}\text{MnO}_3$ and 10 unit cells (39 Å) of $\text{La}_{2/3}\text{Ca}_{1/3}\text{MnO}_3$, with the antiferromagnetic $\text{La}_{1/3}\text{Ca}_{2/3}\text{MnO}_3$ grown first on the substrate. Figure 1 shows the magnetic

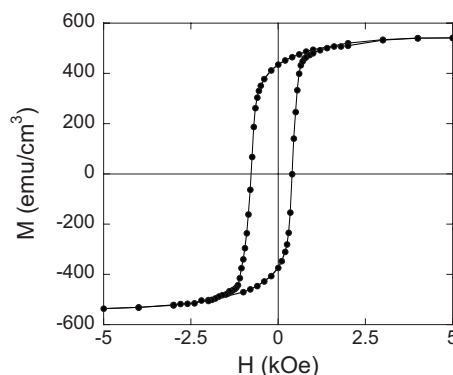


FIG. 1. Magnetic hysteresis loop measured at 10 K after field cooling in 5 kOe. The total magnetization is normalized to the volume of the nominally ferromagnetic layers.

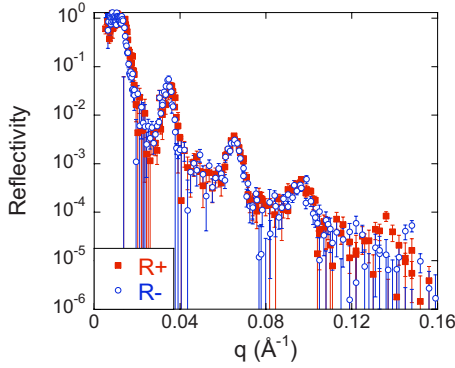


FIG. 2. (Color online). Polarized neutron reflectometry measured at 10 K and 5 kOe. Shown are both nonspin-flip reflectivities R^+ and R^- .

hysteresis loop measured with a superconducting quantum interference device (SQUID) magnetometer at 10 K after field cooling from room temperature in an applied field of 5 kOe. The hysteresis loop shows a clear shift to the left, indicating the exchange-bias of $H_E=220$ Oe in this sample, and the saturation magnetization (normalized to the volume of the nominally ferromagnetic layers) is close to the bulk value of 576 emu/cm^3 and significantly larger than the values typically measured for single layer $\text{La}_{2/3}\text{Ca}_{1/3}\text{MnO}_3$ films ($\approx 400 \text{ emu/cm}^3$).¹⁹

The polarized neutron reflectivity of this sample was measured at the ASTERIX instrument of the Lujan Neutron Scattering Center in the Los Alamos National Laboratory.⁵ The measurements were performed at 5 kOe after field cooling the sample in the same field. Since the applied field was large enough to saturate the sample (see Fig. 1) all of the magnetization is parallel to the applied field, and therefore spin-flip scattering should be absent. Therefore we only polarized the incident neutron beam and measured the reflectivity irrespective of the polarization of the reflected beam. From these measurements we obtain the nonspin-flip crosssections R^+ and R^- , which are shown in Fig. 2 as a function of momentum transfer q . Both reflectivities show clear Bragg reflections, which originate from the superlattice periodicity of 195 Å. Note that for neutron scattering the chemical contrast between $\text{La}_{2/3}\text{Ca}_{1/3}\text{MnO}_3$ and $\text{La}_{1/3}\text{Ca}_{2/3}\text{MnO}_3$ is very small and thus the experimental data is dominated by the magnetic structure and is nearly identical for R^+ and R^- .^{10,20–22}

In order to obtain the magnetization depth profile in our sample we fit the data from Fig. 2 using an iterative Parratt algorithm.^{5,23} The free parameters in this fitting procedure are for each layer their thickness, interface roughness, structural, and magnetic-scattering length densities. In order to constrain the fits further we also measured the x-ray reflectivity using a Phillips XPert diffractometer and fitted that data simultaneously with the polarized neutron reflectivity, as there is little contrast in the nuclear scattering length density for neutrons, but more contrast with the x-rays. Therefore the x-rays were essential for determining the exact chemical structure, such as individual layer thickness and interfacial roughness. Figure 3 shows in the lower panel the polarized neutron reflectivity together with the simulated reflectivities obtained with four different models for the depth dependence

of the magnetization, while keeping the chemical structure identical. In order to clarify any discrepancies between the different models and the experimental data we removed the q dependence due to the Fresnel decay of the reflectivity⁵ by multiplying the reflectivities by q^4 . The upper panel in Fig. 3 shows the magnetization profiles corresponding to the different models for the first bilayer of the superlattice. In each model, the total magnetic moment was constrained to be consistent with the SQUID measurement.

First we investigated model I, which assumes that the magnetization profile is commensurate with the chemical doping profile and that there is no net magnetization in each of the antiferromagnetic layers. As can be seen in Fig. 3 the simulated data reproduce the positions of the superlattice Bragg reflections very well, but with increasing q there are small discrepancies for the intensities in between the Bragg reflections. Next, for models II and III we assumed that the antiferromagnet may have a finite net moment. Net moments in antiferromagnetic layers have been observed in many exchange-bias systems and are believed to be responsible for the shift of the hysteresis loop.^{24–26} First, we considered a homogeneous net moment in the antiferromagnet, since this would naturally explain the increase in the saturation magnetization with increasing antiferromagnetic layer thickness as was observed in Ref. 16. It is evident from Fig. 3 that this model does not improve the fit to the data compared to model I. In fact, the intensities of the Bragg reflections at high q values are significantly underestimated by model II. This can be intuitively understood, since adding an additional magnetization to the antiferromagnetic layer reduces the overall magnetic contrast that the spin-polarized neutrons see, which therefore results in a reduction in the Bragg-peak intensities. For model III we assumed that next to the interface the antiferromagnet develops a net moment extending two unit cells into the antiferromagnet (7.7 Å). In other words the ferromagnetic ordering extends slightly beyond the nominally chemically doped ferromagnetic region. This scenario is very similar to what has been observed for other exchange-bias systems.^{25,26} Yet again, as can be seen in Fig. 3, there is a larger discrepancy between the simulated and experimental data compared to model I, where the magnetization and chemical profiles are commensurate.

Lastly, for model IV we added to model I a net magnetization in the first antiferromagnetic layer, adjacent to the SrTiO_3 substrate. Interestingly, this resulted in a significant improvement of the fit compared to model I. Overall the simulated data of model IV describes the data at high q significantly better and in particular the regions between the Bragg reflections are much better reproduced. This can be qualitatively understood, since the additional ferromagnetic layer gives rise to a long period oscillation in the reflectivity, which adds intensities between the superlattice reflections. Interestingly the magnetization of this ferromagnetically ordered region is comparable to the magnetization in the nominally ferromagnetic layers (see Fig. 3). The thickness of this additional ferromagnetic layer is 30 Å. It should be noted that the presence of a constant ferromagnetic region in the first antiferromagnetic layer is consistent with the experimental observations in Ref. 16, where the normalized saturation magnetization increased with antiferromagnetic layer

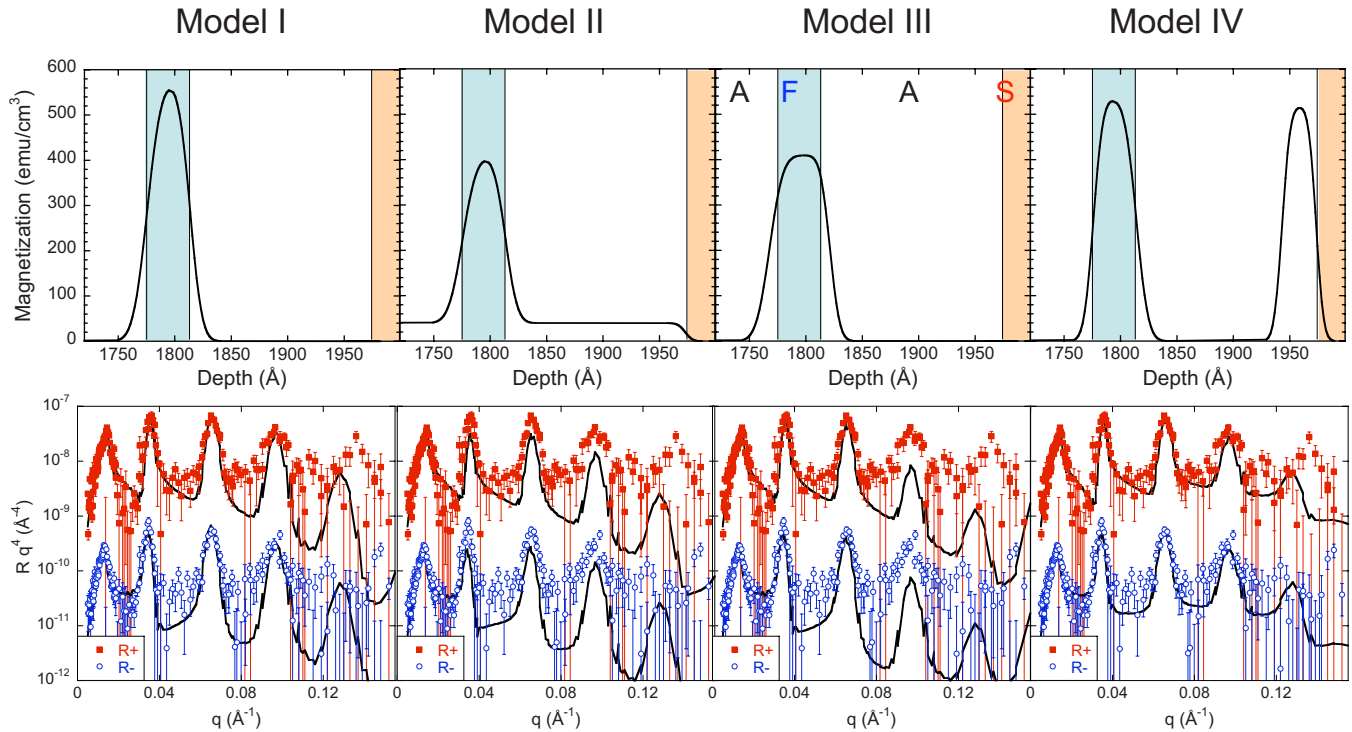


FIG. 3. (Color online). Bottom row: polarized neutron reflectivities R^+ and R^- multiplied by q^4 together with corresponding fits. For clarity R^- is offset by a factor 0.01. Top row: magnetization depth profile of the first superlattice bilayer next to the substrate. A, F, and S mark the nominally antiferromagnetic, ferromagnetic, and substrate regions, respectively. The different models are: (I) magnetization profile commensurate with doping profile and zero magnetization in antiferromagnetic layer; (II) magnetization profile commensurate with doping profile and nonzero magnetization in antiferromagnetic layer; (III) incommensurate magnetization profile with net magnetization extending into the antiferromagnet; and (IV) commensurate magnetization profile with additional net magnetization at the interface between first antiferromagnetic layer and substrate.

thickness. The samples used in Ref. 16 were grown with a constant overall thickness of about 180 nm, so that the number of bilayer repetitions decreased with increasing antiferromagnetic layer thickness.²⁷ This meant that the relative contribution of any net magnetization in the first antiferromagnetic layer also increased for the samples with larger antiferromagnetic layer thickness.

However, the origin for such a ferromagnetically ordered layer next to the substrate interface remains unclear. It is well known that the magnetic properties of manganite films are very sensitive to stress and strain.^{28–30} Therefore, the epitaxial strain may influence the properties of the first layer in the superlattice more than in subsequent layers. For example, in $\text{La}_{0.7}\text{Ca}_{0.3}\text{MnO}_3/\text{YBa}_2\text{Cu}_3\text{O}_7$ heterostructures it was observed that the $\text{La}_{0.7}\text{Ca}_{0.3}\text{MnO}_3$ layer grown on SrTiO_3 had a very different saturation magnetization and coercivity compared to $\text{La}_{0.7}\text{Ca}_{0.3}\text{MnO}_3$ layers further away from the substrate.³¹ Thus it is conceivable that the additional magnetization in the initial antiferromagnetic $\text{La}_{1/3}\text{Ca}_{2/3}\text{MnO}_3$ layer is caused by the epitaxial strain. Additionally, cationic segregation has been observed at $\text{La}_{2/3}\text{Ca}_{1/3}\text{MnO}_3/\text{SrTiO}_3$ interfaces, leading to a reduced Mn valence.³² Such a process would be consistent with the observed ferromagnetic region at the $\text{La}_{1/3}\text{Ca}_{2/3}\text{MnO}_3/\text{SrTiO}_3$ interface. It should be also noted that the epitaxial lattice mismatch with the SrTiO_3 substrate of 2.7% for the antiferromagnetic $\text{La}_{1/3}\text{Ca}_{2/3}\text{MnO}_3$ film is larger than the mismatch of 1.2% for the ferromagnetic

$\text{La}_{2/3}\text{Ca}_{1/3}\text{MnO}_3$ films. Segregation of La cations toward the substrate and Ca cations away from the substrate would reduce this strain.

In order to test these possibilities we measured a single 400-Å thick single layer $\text{La}_{1/3}\text{Ca}_{2/3}\text{MnO}_3$ grown on SrTiO_3 both with SQUID magnetometry and polarized neutron reflectivity after field cooling from room temperature to 10 K in a 5 kOe field. In either measurement there was no indication of a net magnetic moment. However, it is possible that the segregation is kinetically limited and the shorter time of growth of the single layer compared to the superlattice is not sufficient to develop enough Ca deficiency for a net magnetic moment.

In conclusion we have investigated the origin of additional magnetization in antiferromagnetic/ferromagnetic $\text{La}_{1/3}\text{Ca}_{2/3}\text{MnO}_3/\text{La}_{2/3}\text{Ca}_{1/3}\text{MnO}_3$ superlattices by using polarized neutron reflectometry for obtaining the depth profile of magnetization. From the comparison of simulated reflectivities for different plausible models with the polarized neutron reflectometry data we find that contrary to the assumption in Ref. 16 the excess magnetization does not occur at the $\text{La}_{1/3}\text{Ca}_{2/3}\text{MnO}_3/\text{La}_{2/3}\text{Ca}_{1/3}\text{MnO}_3$ interfaces, but instead an additional layer with a net magnetization develops within the first antiferromagnetic $\text{La}_{1/3}\text{Ca}_{2/3}\text{MnO}_3$ layer at its interface with the SrTiO_3 substrate. The exact origin of this additional net magnetization remains unclear, but most likely epitaxial strain and/or charge transfer at the interfaces are important.

This work was supported by the U.S. Department of Energy—Basic Energy Science under Contract No. DE-AC02-06CH1357 at Argonne National Laboratory and DE-AC52-06NA25396 at Los Alamos National Laboratory and

by COLCIENCIAS under the Excellence Center for Novel Materials, Contract No. 043-2005. S.P. was supported from KOSEF (R01-2008-000-21092-0) and (KRF-2006-005-J02803).

*hoffmann@anl.gov

- ¹E. Dagotto, *Science* **318**, 1076 (2007).
- ²A. P. Ramirez, *Science* **315**, 1377 (2007).
- ³F. Ott, M. Viret, R. Borges, R. Lyonnet, E. Jacquet, C. Fermon, and J. P. Contour, *J. Magn. Magn. Mater.* **211**, 200 (2000).
- ⁴M. R. Fitzsimmons *et al.*, *J. Magn. Magn. Mater.* **271**, 103 (2004).
- ⁵M. R. Fitzsimmons and C. F. Majkrzak, in *Modern Techniques for Characterizing Magnetic Materials*, edited by Y. Zhu (Springer, New York, 2005), Chap. 3, pp. 107–155.
- ⁶A. Hoffmann, S. G. E. te Velthuis, Z. Sefrioui, J. Santamaría, M. R. Fitzsimmons, S. Park, and M. Varela, *Phys. Rev. B* **72**, 140407(R) (2005).
- ⁷J. Stahn *et al.*, *Phys. Rev. B* **71**, 140509(R) (2005).
- ⁸D. Niebieskikwiat, L. E. Hueso, J. A. Borchers, N. D. Mathur, and M. B. Salamon, *Phys. Rev. Lett.* **99**, 247207 (2007).
- ⁹F. Ott, *J. Phys.: Condens. Matter* **20**, 264009 (2008).
- ¹⁰S. J. May, A. B. Shah, S. G. E. te Velthuis, M. R. Fitzsimmons, J. M. Zuo, X. Zhai, J. N. Eckstein, S. D. Bader, and A. Bhattacharya, *Phys. Rev. B* **77**, 174409 (2008).
- ¹¹W. Meiklejohn and C. Bean, *Phys. Rev.* **102**, 1413 (1956).
- ¹²J. Nogués, J. Sort, V. Langlais, V. Skumryev, S. Suriñach, J. S. Muñoz, and M. Baró, *Phys. Rep.* **422**, 65 (2005).
- ¹³I. Panagiotopoulos, C. Christides, N. Moutis, M. Pissas, and D. Niarchos, *J. Appl. Phys.* **85**, 4913 (1999).
- ¹⁴I. Panagiotopoulos, C. Christides, D. Niarchos, and M. Pissas, *J. Appl. Phys.* **87**, 3926 (2000).
- ¹⁵N. Moutis, C. Christides, I. Panagiotopoulos, and D. Niarchos, *Phys. Rev. B* **64**, 094429 (2001).
- ¹⁶G. Campillo, A. Hoffmann, M. E. Gomez, and P. Prieto, *J. Appl. Phys.* **97**, 10K104 (2005).
- ¹⁷M. B. Salamon and M. Jaime, *Rev. Mod. Phys.* **73**, 583 (2001).
- ¹⁸A. Ohtomo, D. A. Muller, J. L. Grazul, and H. Y. Hwang, *Nature* (London) **419**, 378 (2002).
- ¹⁹G. Campillo, A. Berger, J. Osorio, J. Pearson, S. Bader, E. Baca, and P. Prieto, *J. Magn. Magn. Mater.* **237**, 61 (2001).
- ²⁰G. P. Felcher, K. E. Gray, R. T. Kampwirth, and M. B. Brodsky, *Physica B & C* **136**, 59 (1986).
- ²¹A. Hoffmann, M. R. Fitzsimmons, J. A. Dura, and C. F. Majkrzak, *Phys. Rev. B* **65**, 024428 (2001).
- ²²M. Vadalá, K. Zhernenkov, M. Wolff, B. P. Toperverg, K. Westerholt, H. Zabel, P. Wisniewski, S. Cardoso, and P. P. Freitas, *J. Appl. Phys.* **105**, 113911 (2009).
- ²³L. G. Parratt, *Phys. Rev.* **95**, 359 (1954).
- ²⁴K. Takano, R. H. Kodama, A. E. Berkowitz, W. Cao, and G. Thomas, *Phys. Rev. Lett.* **79**, 1130 (1997).
- ²⁵A. Hoffmann, J. W. Seo, M. R. Fitzsimmons, H. Siegart, J. Fompeyrine, J.-P. Locquet, J. A. Dura, and C. F. Majkrzak, *Phys. Rev. B* **66**, 220406(R) (2002).
- ²⁶S. Roy *et al.*, *Phys. Rev. Lett.* **95**, 047201 (2005).
- ²⁷G. Campillo, A. Hoffmann, M. E. Gómez, and P. Prieto, *Rev. Colomb. Fís.* **37**, 215 (2005).
- ²⁸A. J. Millis, T. Darling, and A. Migliori, *J. Appl. Phys.* **83**, 1588 (1998).
- ²⁹T. Wu, S. B. Ogale, S. R. Shinde, A. Biswas, T. Polletto, R. L. Greene, T. Venkatesan, and A. J. Millis, *J. Appl. Phys.* **93**, 5507 (2003).
- ³⁰X. J. Chen, S. Soltan, H. Zhang, and H.-U. Habermeier, *Phys. Rev. B* **65**, 174402 (2002).
- ³¹V. Peña, Z. Sefrioui, D. Arias, C. Leon, J. Santamaría, J. L. Martínez, S. G. E. te Velthuis, and A. Hoffmann, *Phys. Rev. Lett.* **94**, 057002 (2005).
- ³²S. Estradé, J. Arbiol, F. Peiró, I. C. Infante, F. Sánchez, J. Fontcuberta, F. de la Peña, M. Walls, and C. Colliex, *J. Appl. Phys. Lett.* **93**, 112505 (2008).